Real Space Investigation of the Roughening and Deconstruction Transitions of Au(110)

M. Sturmat, R. Koch, and K. H. Rieder

Institut für Experimentalphysik, Freie Universität Berlin, Arnimallee 14, D-14195 Berlin, Germany

(Received 13 August 1996)

As established by diffraction techniques Au(110)-(1 × 2), which is missing-row reconstructed at 300 K, consecutively undergoes two phase transitions upon heating: an Ising transition at ≈650 K and a 3D roughening transition at ≈700 K. Our teal space investigation with atomic scale resolution by temperature-variable scanning tunneling microscopy reveals that—contrary to present theoretical models—the Ising transition is due to antiphase domains developing during the 2D roughening of (1 × 3) steps. The missing-row configuration of interior terrace regions remains completely stable until the 3D roughening temperature, thus ruling out an order-disorder transition via lattice gas formation. [S0031-9007(96)01915-1]

PACS numbers: 61.50.Ks, 61.16.Ch, 68.35.Bs, 82.65.Dp

Owing to the superior experimental and theoretical standards of surface sciences and thin film technology it nowadays has become feasible to prepare high quality 2D (two-dimensional) systems with long-range periodic order over distances of several hundred nanometers. From a theoretical point of view it is known at least since the celebrated solution of the 2D Ising model by Onsager [1] that 2D systems—as their counterparts 3D—can undergo phase transitions [2]. Until now several other 2D models have been solved exactly with the methods of statistical mechanics, but the number of experimental realizations of such model systems still is minute. Recently fcc(110) surfaces [Fig. 1(a)], aside from their importance for catalysis, have attracted considerable interest for the study of phase transitions in 2D. Though discussed controversially for many years, it is now well established that fcc(110) surfaces of transition metals exhibit a pronounced tendency to reconstructions of the MR (missing-row) type either in the clean state or driven by adsorbates [3]. More recently another characteristic feature of fcc(110) surfaces has been discovered, namely, that they undergo a 3D roughening transition at temperatures well below the bulk melting point (see reviews of Refs. [4,5]), which for the unreconstructed surfaces is of the Kosterlitz-Thouless type [6]. In the case of Au(110) and Pt(110), which are (1 × 2) MR reconstructed already in the ground state [Fig. 1(b)], the situation is even more complex, as on these two surfaces the processes of deconstruction and roughening are coupled [7]. Whereas on Pt(110) both processes proceed at the same temperature [8], for Au(110) an additional phase transition has been identified from the disappearance of the half-order diffraction spots [9–13]. The respective transition temperature T_C given in literature varies between 650 and 735 K, but in any case lies about 50 K below the roughening temperature T_R. The critical exponents at T_C are in accordance with the 2D Ising universality class [1]. Up to now, however, there is still controversy about the structural models, particularly for the Ising transition [4]. On the basis of Monte Carlo simulations Campuzano *et al.* [14] suggested a 2D order-disorder transition characterized by random distribution of the topmost half-layer Au atoms between original and missing-row sites [i.e., both sites of the same type, Fig. 1(b)]. The main defects near T_C therefore are the domain walls between the (1 × 2) MR patches [Figs. 1(c) and 1(d)]. More refined models additionally include the possibility of step excitations [15] [Figs. 1(e) and 1(f)] and step-step interactions as well. As discussed by Vilfan and Villain [16], for strong interaction between a pair of opposite (1 × 3) steps [e.g., Fig. 1(g)] the surface undergoes first an Ising and at higher temperatures a roughening transition. In the case of weak interaction, on the other hand, deconstruction and roughening occur at the same temperature. According to a cell-spin model of den Nijs [7], which is based on semi-infinite (1 × 2) MR stripes separated by domain walls or steps [Figs. 1(c)–1(f)], roughening induces simultaneous deconstruction, when the wall energy exceeds twice the value of steps, though still exhibiting Ising exponents. So far, however, a conclusive study that unambiguously

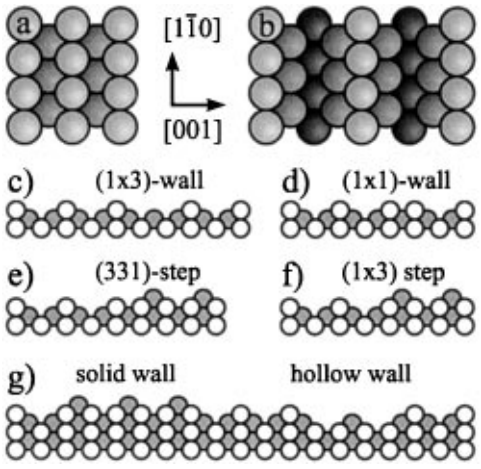

FIG. 1. Top view sphere models of (a) the fcc(110) surface and (b) fcc(110)-(1 × 2) with every other close-packed row missing. (c)–(g) Side view sphere models (i.e., in the [1$\bar{1}$0] direction) of thermal excitations of fcc(110)-(1 × 2).

distinguishes between the different models is still lacking. As is well known, diffraction techniques very accurately determine the critical exponents of phase transitions, but the structural information obtained in reciprocal space is not unequivocally transformed into real space.

Here we report on a scanning tunneling microscopy (STM) investigation of the phase transitions of Au(110)-(1×2), performed *in situ* with a temperature-variable STM at 300–700 K. Real space imaging with atomic scale resolution discloses many details of both the proposed order-disorder and roughening transitions. In contrast to the predictions of the theoretical models discussed above the (1×2) MR configuration is stable up to the roughening temperature. Moreover, in all models the paramount role of [001] steps [compare Fig. 3(b)] for disorder and roughening processes unquestionably has been underestimated so far.

The experiments were performed in an ultrahigh vacuum (UHV) chamber (base pressure $<1 \times 10^{-10}$ mbar) equipped with a temperature-variable UHV-STM, LEED, and the usual facilities for sample preparation [17]. The sample holder of our home-built STM [17] includes a resistively heated oven onto which the sample is mounted. The heater can be operated on the manipulator for preparation as well as in the position of the STM tip, where reliable STM experiments at temperatures of presently up to $\approx$1000 K are possible. Thermal drift converges to tolerable values within 30–45 min after the heating current has been changed. The Au(110) sample, which was investigated already in a previous study [17], was prepared by repeated cycles of Ne sputtering and heating to 670 K, until sharp LEED patterns of Au(110)-(1×2) were obtained. At room temperature the sample exhibits extended (1×2) reconstructed terraces [Fig. 2(a)] with dimensions that point to a miscut angle of less than 0.5°. For the experiments at elevated temperatures the sample was transferred to the STM immediately after preparation and heated to the appropriate temperature T_S. The values of T_S given in the text are accurate to within $\pm$30 K. All STM images were taken in the constant current mode at tip voltages U_T and tunneling currents I_T specified in the respective figure captions.

Figure 2(a) shows an STM top view image of Au(110) near room temperature. In good agreement with previous studies (e.g., [18]) the surface is characterized by well ordered (1×2) MR reconstructed terraces that extend over several 100 nm in the $[1\bar{1}0]$ direction and 10–50 nm along [001]. Terraces are separated almost exclusively by steps of single height, whereby the steps preferentially run parallel to the close-packed rows [i.e., along $[1\bar{1}0]$, type Fig. 1(f)]. Au atoms located at kink sites are quite mobile even at room temperature [19] as is indicated by respective structural changes occurring at [001] steps from scan to scan. Heating the sample to $\approx$420 K significantly increases edge diffusion in the $[1\bar{1}0]$ direction. Figure 2(b) displays a respective section with narrow terraces. Steps still predominantly have $[1\bar{1}0]$ orientation, but now the step edges are composed of many small segments of close-packed rows. Moreover, the segments are not stable concerning both their actual position and length [20]. The corrugation visible in some of the segments [e.g., A in Fig. 2(b)] indicates that single mobile Au atoms were imaged in Fig. 2(b), though part of the step instability may arise from the scanning tip itself. Occasionally a Au atom is trapped by the STM tip for one or two (1×2) MR periods; this explains why sometimes the corrugation of adjacent lower terraces appears to be raised by monostep height to the next terrace [B in Fig. 2(b)]. Upon further increase of the temperature [Figs. 2(c) and 2(d)] the smooth edges of $[1\bar{1}0]$ steps have disappeared completely. The respective step profile is jagged and locally characterized by irregular sawtooth and fjordlike shapes. Figure 3(a) shows single sawteeth at higher magnification. Obviously both the sawteeth and the area of the lower terraces surrounding them are (1×2) MR reconstructed. Since considerable mass transport is necessary to create

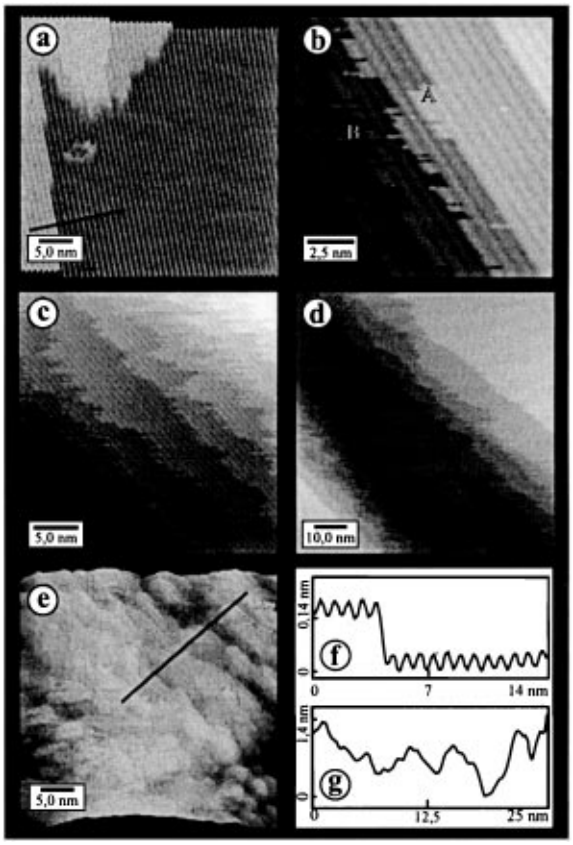

FIG. 2. *In situ* STM images illustrating the two phase transitions of Au(110)-(1×2) in real space: (a) $\approx$300 K, (b) $\approx$420 K, (c) $\approx$550 K, (d) $\approx$620 K, (e) $\approx$700 K, (f) and (g) single scans along dashed lines marked in (a) and (e), respectively. Images (a) and (e) are illuminated, (b)–(d) greyscale top views with black (white) being low (high); $U_T = -826$ mV and $I_T = 5$ nA.

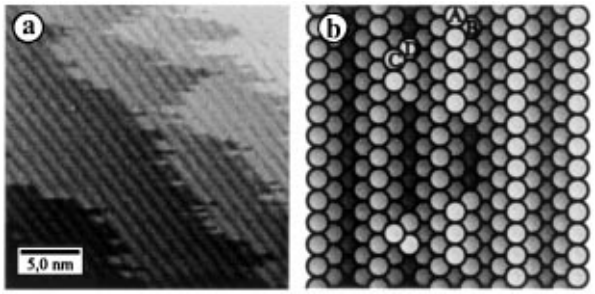

FIG. 3. (a) *In situ* high resolution STM image of jagged step profiles on Au(110)-(1 × 2) at ≈550 K [Figs. 2(c) and 2(d)]; notice the perfect (1 × 2) MR periodicity at and around the sawtoothlike shapes and of inner terrace regions; $U_T = -826$ mV, $I_T = 5$ nA. (b) Schematic illustration of the 2D roughening of an originally straight (1 × 3) step (A) by atom movement from rows A and B to rows C and D. Notice that this restructuring necessitates only terrace and step-down diffusion.

the jagged step configuration while preserving MR geometry, the observed step morphology of Figs. 2(c) and 2(d) certainly is not an experimental artifact generated by the STM tip. A possible model for the 2D roughening is displayed in Fig. 3(b). Notice that in order to grow sawteeth out of a previously straight (1 × 3) step (marked by A), the *missing* rows of the underlying terrace necessarily have to be refilled with Au atoms. For the structural rearrangement sketched in Fig. 3(b) only neighboring atoms participate and diffusion proceeds exclusively on the (110) terraces or downward the (1 × 3) steps; i.e., no upward hopping is involved. Large scale STM images taken at ≈620 K additionally reveal the presence of extended terraces with dimensions similar to the room temperature surface, indicating that the average density of (1 × 3) steps remains nearly constant upon raising the temperature. A closer look [Fig. 4(a)] to the broad terrace located in the center of Fig. 2(d) reveals that interior terrace regions are still perfectly (1 × 2) MR reconstructed, thus underlining the remarkable stability of the (1 × 2) MR configuration even at about ≈620 K. After heating the sample to ≈700 K flat (110) terraces no longer are detected [Fig. 2(e)]. The surface consists of irregular mounds with lateral and vertical dimensions of several nanometers, thus demonstrating roughening in 3D. We remark that the structural features presented above did not depend on whether the sample temperature T_S was reached by heating or cooling indicating that—in agreement with the previous diffraction studies [9–13]—they represent equilibrium at T_S. A substantial influence on surface impurities can also be excluded, particularly because the observed morphology is not a local phenomenon but representative for the sample at T_S. As shown by McRae *et al.* [21] surface segregation of Sn, which leads to a decrease of T_C, requires prolonged annealing of the sample at temperatures of 700–800 K, i.e., significantly higher than the temperatures used in the present investigation. STM itself, which has proven in the past to be a sensitive detector for small amounts of impurities as well, indicates contamination values less than 0.1%.

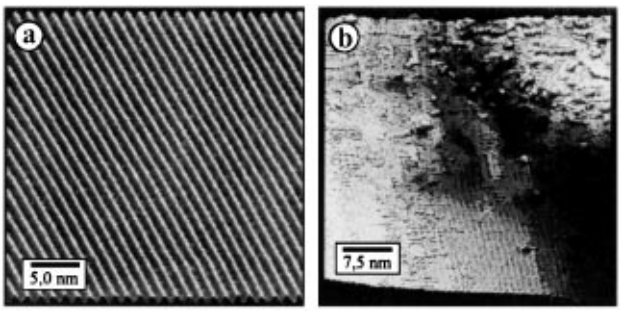

FIG. 4. *In situ* high resolution STM top view images of Au(110)-(1 × 2) of (a) the perfect (1 × 2) MR configuration inside extended terraces at ≈620 K [Fig. 2(d)] and (b) coexisting (1 × 2) MR reconstructed terraces (lower half) and 3D rough areas (upper half) near the roughening transition (≈700 K); $U_T = -826$ mV, $I_T = 3$ nA.

The scenario of the disordering of Au(110)-(1 × 2) 2D and 3D visualized *in situ* by STM certainly is at variance with the present theoretical models of deconstruction and roughening. The order-disorder transition via lattice gas formation proposed by Campuzano *et al.* [14] definitely can be excluded. Our STM results unambiguously demonstrate that disorder processes preceding 3D roughening are confined to step edges, whereby the (1 × 2) MR configuration of interior terrace regions [Fig. 4(a)], but also at the step edges itself definitely remains stable until 3D roughening sets in [Fig. 3(a)]. This point is further corroborated by the STM image of Fig. 4(b) of the Au surface close to T_R (≈650 K). Whereas in the upper half 3D mounds with dimensions of several nm have developed, the flat terraces of the lower half still exhibit the (1 × 2) MR periodicity. Notice also the absence of (1 × 2) MR structures on the mounded region, which is in accordance with the predictions of den Nijs [7] that on fcc(110) surfaces *3D roughening induces a simultaneous deconstruction transition.*

Another feature predicted essentially by all theoretical models, but not approved by our STM results concerns the increase of $[1\bar{1}0]$ domain walls [e.g., Figs. 1(c) and 1(d)] or $[1\bar{1}0]$ steps [e.g., Figs. 1(e) and 1(f)] near the disorder transition at T_C. Whereas the simple Ising domain walls of Figs. 1(c) and 1(d), which should form inside broader terraces, are not observed at all (see discussion above), the average density of (1 × 3) steps remains constant within experimental accuracy up to the roughening transition at T_R. Between 400–600 K, however, a dramatic increase of [001] steps [Figs. 2(c), 2(d), and 3] is observed, which gives rise to the jagged appearance of the step profiles. Both findings are in agreement with the x-ray diffraction study of Keane *et al.* [11]. They concluded that at the Ising phase transition of Au(110)-(1 × 2) surface *undergoes a reversible deconstruction transition*

characterized by a proliferation of compact antiphase defects [along $[1\bar{1}0]$ as displayed in Figs. 1(c) and 1(d)] *with no measurable change in the density of surface steps.* Our STM results, however, clearly reveal that the antiphase defects preferentially occur in the [001] direction rather than along $[1\bar{1}0]$.

On the basis of our real space investigation we suggest the following two-stage mechanism for roughening on Au(110)-(1×2): (i) Because of the unavoidable miscut present in any human made surface, terraces generally are finite sized and consequently separated by steps. On Au(110)-(1×2) upon increasing temperature in a first stage the free energy of (1×3) steps vanishes in comparison with kinks, i.e., [001] steps. As a result, steps no longer preferentially run parallel to the close-packed rows, but are composed in the irregular manner of small $[1\bar{1}0]$ and [001] segments. In this stage terraces still are flat and (1×2) MR reconstructed, though exhibiting jagged boundaries. The 2D roughening of step edges on Au(110)-(1×2) resembles the structural model proposed by den Nijs *et al.* [22] for the roughening of vicinal (11 m) surfaces of fcc metals, where the steps *assume fractal structures and meander like coastlines.* However, whereas the roughening transition of the (11 m) surfaces is of the Kosterlitz-Thouless type, the fact that Au(110)-(1×2) and *and* stays reconstructed during step roughening favors an Ising transition for the disappearance of half-order diffraction spots. In the step-pairing model of Vilfan and Villain [23], which originally was proposed to account for the Ising criticality of Pt(110)-(1×2), pairs of steps are bound together and represent the Ising domain walls. As illustrated in Fig. 1(g) the corresponding Ising domains are (1×2) MR stripes of neighboring terraces. As in the "disordered flat phase" of Rommelse and den Nijs [24] the surface remains flat on average and is characterized by a long-range up-down order. Our experiments indeed reveal a similar Ising configuration at the jagged step edges, which divide the surface in small (1×2) MR patches located on upper and lower terraces, respectively [Fig. 3(b)]. The Ising domain walls are formed by pairs of steps of the sawtooth structure. As the process of 2D step roughening is confined to preexisting steps, it probably explains the large scattering of the Ising transition temperature given in the literature, since the step density strongly depends on crystal quality and preparation. (ii) In a second stage, when the free energy for the creation of steps vanishes at higher temperatures, the surface roughens in three dimensions and simultaneously deconstructs.

In conclusion, the *in situ* investigation of Au(110)-(1×2) with a variable-temperature STM provides a comprehensive picture for the two phase transitions observed previously by diffraction methods. The real space imaging of step roughening in 2D as well as 3D roughening and simultaneous deconstruction of Au(110), though only incompletely described by present models, certainly improves our understanding of phase transitions. It therefore hopefully will stimulate future theoretical and experimental studies, including Pt(110) and Ir(110), on this interesting and important topic.

[1] L. Onsager, Phys. Rev. **65**, 117 (1944).

[2] I. Lyuksyutov, A. G. Naumovets, and V. Pokrovsky, *Two-Dimensional Crystals* (Academic Press, Inc., Boston, 1992).

[3] Review article by R. Koch, M. Borbonus, O. Haase, and K. H. Rieder, Appl. Phys. A **55**, 417 (1992), and references therein.

[4] Review articles by M. den Nijs or K. Kern or J. C. Campuzano, in *Phase Transitions and Adsorbate Restructuring at Metal Surfaces*, The Chemical Physics of Solid Surfaces Vol. 7, edited by D. A. King and D. P. Woodruff (Elsevier, Amsterdam, 1994), and references therein.

[5] Review article by M. Bernasconi and E. Tosatti, Surf. Sci. Rep. **17**, 363 (1993), and references therein.

[6] J. M. Kosterlitz and D. J. Thouless, J. Phys. C **6**, 1181 (1973); J. M. Kosterlitz, J. Phys. C **7**, 1046 (1974).

[7] M. den Nijs, Phys. Rev. Lett. **66**, 907 (1991).

[8] I. K. Robinson, E. Vlieg, and K. Kern, Phys. Rev. Lett. **63**, 2578 (1989).

[9] D. Wolf, H. Jagodzinski, and W. Moritz, Surf. Sci. **77**, 265 (1978).

[10] J. C. Campuzano, M. S. Foster, G. Jennings, R. F. Willis, and W. N. Unertl, Phys. Rev. Lett. **54**, 2684 (1985).

[11] D. T. Keane, P. A. Bancel, J. L. Jordan-Sweet, G. A. Held, A. Mak, and R. J. Birgeneau, Surf. Sci. **250**, 8 (1991).

[12] J. Sprösser, B. Salanon, and J. Lapujoulade, Europhys. Lett. **16**, 283 (1991).

[13] D. Cvetko, A. Lausi, A. Morgante, F. Tommasini, and K. C. Prince, Surf. Sci. **269/270**, 68 (1992).

[14] J. C. Campuzano, A. M. Lahee, and G. Jennings, Surf. Sci. **152/153**, 265 (1978).

[15] J. Villain and I. Vilfan, Surf. Sci. **199**, 165 (1988); G. Mazzeo, G. Jug, A. C. Levi, and E. Tosatti, Surf. Sci. **273**, 237 (1992).

[16] I. Vilfan and J. Villain, Surf. Sci. **257**, 368 (1991).

[17] O. Haase, M. Borbonus, R. Koch, P. Muralt, and K. H. Rieder, Sci. Instrum. **61**, 1480 (1990).

[18] J. K. Gimzewski, R. Berndt, and R. R. Schlittler, Phys. Rev. B **45**, 6844 (1992).

[19] J. K. Gimzewski, R. Berndt, and R. R. Schlittler, Surf. Sci. **247**, 327 (1991); S. Speller, S. Molitor, C. Röthig, J. Bömermann, and W. Heiland, Surf. Sci. **312**, L748 (1994).

[20] L. Kuipers, M. S. Hoogeman, J. W. M. Frenken, and H. van Beijeren, Phys. Rev. B **52**, 11 387 (1995).

[21] E. G. McRae, T. M. Buck, R. A. Malic, and G. H. Wheatley, Phys. Rev. B **36**, 2341 (1987).

[22] M. den Nijs, E. K. Riedel, E. H. Conrad, and T. Engel, Phys. Rev. Lett. **55**, 1689 (1985).

[23] I. Vilfan and J. Villain, Phys. Rev. Lett. **65**, 1830 (1990).

[24] K. Rommelse and M. den Nijs, Phys. Rev. Lett. **59**, 2578 (1987); M. den Nijs, Phys. Rev. Lett. **64**, 435 (1990).